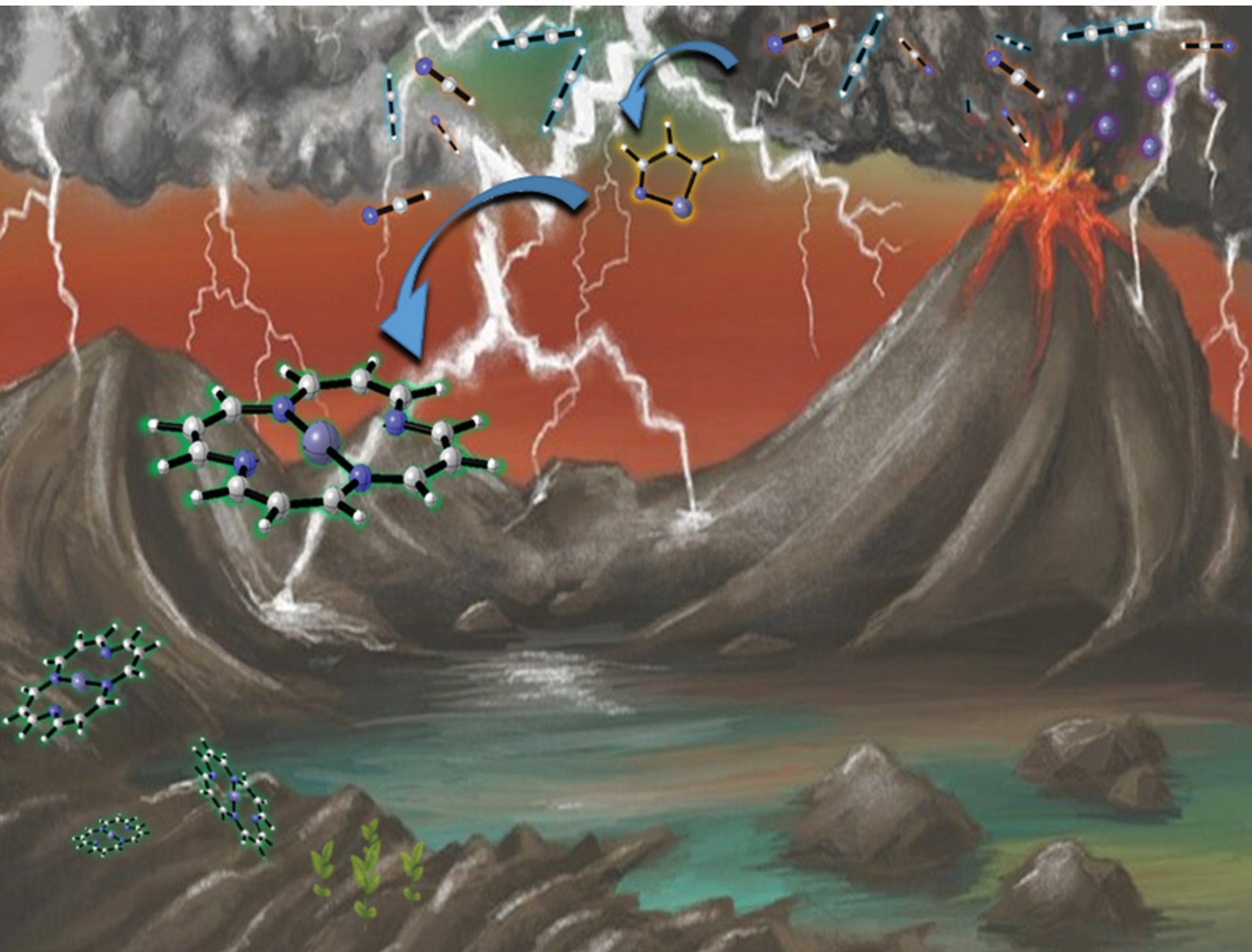


PCCP

Physical Chemistry Chemical Physics
rsc.li/pccp



ISSN 1463-9076



Cite this: *Phys. Chem. Chem. Phys.*,
2022, 24, 16979

Phot0, a plausible primeval pigment on Earth and rocky exoplanets[†]

Juan García de la Concepción, ^a Luis Cerdán, ^b Pablo Marcos-Arenal, ^a Mercedes Burillo-Villalobos, ^c Nuria Fonseca-Bonilla, ^a Rubén Lizcano-Vaquero, ^d María-Ángeles López-Cayuela, ^e José A. Caballero, ^f and Felipe Gómez ^a

In view of the existing controversy around the origin of the photosynthesis and, therefore, the first photosynthetic pigments, our work focuses on the theoretical study of a hypothetical first pigment, simpler than those existing today, that collects energy from solar radiation on Earth-like exoplanets. Our theoretical results show that there could exist geochemical conditions that allow the abiotic formation of a primeval pigment that might become sufficiently abundant in the early stages of habitable rocky exoplanets. These conditions would place this pigment before the appearance of life in a very young planet, thanks to chemical routes instead of biochemical transformations. Thus, our results may refute the currently accepted hypothesis that the complex biomolecules that allowed the photosynthesis to be carried out were synthesized through complex and evolved metabolic pathways. In addition, we show that the proposed primeval pigment, which we call Phot0, is also a precursor of the more evolved pigments known today on Earth and demonstrate, for the first time, an abiotic chemical route leading to tetrapyrroles not involving pyrrole derivatives. Our proposal places simple and very abundant raw materials in never-before-proposed geochemical conditions that lead to the formation of biomolecules of biological interest.

Received 12th April 2022,
Accepted 13th June 2022

DOI: 10.1039/d2cp01703b

rsc.li/pccp

1 Introduction

The origin of photosynthesis and its pigments is a hotly debated topic on which there is still no clear consensus.^{1,2} Some authors consider that the photosynthesis and the origin of life were contemporary during the prebiotic phase,^{3,4} while others favor a photosynthesis occurrence much later than the origin of life.^{5,6} In the late occurrence scenario, photosynthesis appeared in bacteria containing DNA, ATP synthase, and electron transport proteins, which are very evolved organisms. However, even advocates of an early photosynthesis occurrence

place the chlorophylls and bacteriochlorophylls as the first pigments of the light-harvesting complexes.

Within the theory of common ancestors, it is proposed that many molecules of great interest such as proteins, RNA, and membranes, should have been much simpler than those present in modern cells. In this sense, it is hypothesized that there should have existed simple oligopeptides and oligonucleotides, as well as simple alkyl amphiphilic hydrocarbons, as primeval membranes.⁷ Today, evolved cells obtain essential biomolecules through complex metabolic routes, but it is suspected that these complex metabolic pathways were not present in the first ancestors. Indeed, it has been proposed that the catalysts of the photosynthesis such as chlorophylls and bacteriochlorophylls should have come from simple organic compounds.⁸ The question of whether these simple compounds served as photosynthetic pigments does not have an answer yet.

The idea of a simple primitive pigment arises from the chemical structure observation of the most evolved pigments. Current chlorophylls and bacteriochlorophylls are tetrapyrrolic pigments needed to carry out the photosynthesis, but the structure of these macrocycles is very similar to that of other biomolecules such as the heme groups (A, B, C, or O) present in hemoglobin, myoglobin, peroxidases, cyclooxygenases, cytochrome C, or cytochrome P450. All these biomolecules are

^a Centro de Astrobiología (CSIC-INTA), Ctra. de Ajalvir km. 4, Torrejón de Ardoz, 28850 Madrid, Spain. E-mail: jgarcia@cab.inta-csic.es

^b Instituto de Ciencia Molecular (ICMol), Universidad de Valencia, 46071 Valencia, Spain

^c Ingeniería de Sistemas para la Defensa de España (ISDEFE), 28040 Madrid, Spain

^d Universidad Autónoma de Madrid, Ciudad Universitaria de Cantoblanco, 28049, Madrid, Spain

^e Instituto Nacional de Técnica Aeroespacial (INTA), Atmospheric Research and Instrumentation Branch, 28850 Torrejón de Ardoz, Madrid, Spain

^f Centro de Astrobiología (CSIC-INTA), European Space Astronomy Centre, Camino bajo del Castillo, 28691 Villanueva de la Cañada, Madrid, Spain

† Electronic supplementary information (ESI) available: Detailed explanation of the reaction mechanism for the formation of Phot0 and cycloaddition reactions. Cartesian coordinates for all the optimized geometries. See DOI: <https://doi.org/10.1039/d2cp01703b>



derived from porphyrin, chlorin, bacteriochlorin, or isobacteriochlorin. Olson *et al.*^{1,2} placed chlorophyll biosynthesis from uroporphyrinogen and uroporphyrin, also tetrapyrrole derivatives. The presence of these complex macrocycles in a multitude of biological structures, as well as in all photosynthetic organisms, leads us to think that, as it happened with the primeval membranes, oligopeptides, and oligonucleotides, these tetrapyrroles were too evolved as to have been present since the origin of the photosynthesis. According to the proposed abiotic chemical routes for the formation of tetrapyrrole macrocycles,^{9–11} the condensation of pyrrole derivatives is mandatorily required. These syntheses need many chemical species and steps,¹² catalysts,¹³ and, in some cases, highly functionalized pyrroles.^{9–11,14–16} The latter are too complex to be present in large concentrations on such a primeval rocky planet. This scenario points out that the concentration of pyrrole and tetrapyrrole derivatives in the primeval Earth environment should have been low.

In this work, we propose a chemical route towards a simple and primitive photosynthetic pigment, namely Phot0, in geochemical conditions not considered so far. In addition, our new metric for quantifying the photosynthetic activity fitness¹⁷ suggests that Phot0 could be useful as a photosynthetic pigment in reducing atmospheres like that of the early Earth. Finally, we demonstrate that Phot0 could be a precursor of the tetrapyrrolic pigments known today thanks to chemical routes that do not involve the condensation of complex pyrroles.

2 Results and discussion

2.1 The Phot0 system

The aim of this work is to find a simple and primeval light-harvesting pigment of the photosynthetic common ancestor. The only part of the carbon backbone that all the tetrapyrrole derivatives share is the central macrocycle surrounding the metal cation, in particular, the (1E,2Z,4E,6Z,8E,10-Z,12E,14Z)-1,5,9,13-tetraazacyclohexadeca-2,4,6,8,10,12,14,16-octaene, referred herein as **16- π -TAzCy** (Fig. 1a). The structure of this conjugated tetraazacycle displays 16 π delocalized electrons, being an antiaromatic compound. This antiaromatic character, together with the imine bonds of the macrocycle, should entail a marked instability against water, making it susceptible to be hydrolyzed. The reduction of **16- π -TAzCy** by two electrons would lead to the 18- π -aromatic heterocycle **18- π -TAzCy²⁻**. This reducing character could be provided by a divalent metal in oxidation state 0. This kind of metals, such as Fe and Mg, are quite abundant in protoplanetary disks and, therefore, rocky exoplanets, and would give rise to the coordination compound **M-18- π -TAzCy** (Fig. 1a).

Fig. 1b and c show two tentative chemical routes leading to the **M-18- π -TAzCy**-type aromatic compound. The most intuitive path is the reduction of **16- π -TAzCy** by a divalent metal. Considering that our synthetic proposals should fit in the early Earth conditions, that reduction should take place in an environment without liquid water. Since the volcanic activity

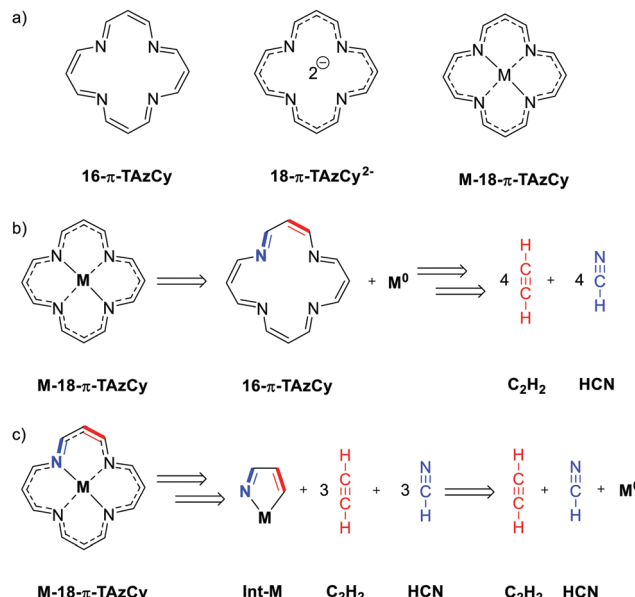


Fig. 1 Structural and retrosynthetic analyses of the central ring of tetrapyrrole derivatives. (a) Chemical structure of **16- π -TAzCy**, **18- π -TAzCy²⁻** and **M-18- π -TAzCy**. (b) Retrosynthetic analysis of **M-18- π -TAzCy** considering **16- π -TAzCy** as a precursor. (c) Retrosynthetic analysis of **M-18- π -TAzCy** considering the chelate complex **Int-M** as intermediate.

on the primitive Earth was very high, the liquid water must have shown a considerably low pH.¹⁸ Therefore, metals such as Cu or Zn (non-reactive in neutral water) would react with the protons of the acidic solutions, generating **H₂** and metallic cations that, in turn, would react to end up as hydroxides. On the other hand, highly reducing metals such as alkaline earth metals would react rapidly in water generating the hydroxide and **H₂**.¹⁹

A retrosynthetic analysis of **16- π -TAzCy** leads to acetylene, **C₂H₂**, and hydrogen cyanide, **HCN**, (Fig. 1b), which are two highly abundant molecules in the interstellar medium.^{20,21} In fact, it has been shown that **C₂H₂** and **HCN** are also formed in volcanic processes²². Indeed, **C₂H₂** and **HCN** are very related to each other in reducing atmospheres of earth-like exoplanets since the abundance of **HCN** strongly depends on the abundance of carbon-bearing gasses such as **C₂H₂**.²³ Also, typical phenomena of a primitive Earth such as electric discharge conditions and impactors in reducing conditions have been shown to produce high amounts of **HCN**.^{24–27}

The expected high abundance of **C₂H₂** and **HCN** in the reducing atmosphere of the primeval Earth narrows down the possibilities towards physical conditions typical of the gas phase. The only possibility of finding neutral metals in the gas phase in nature is in volcanic eruptions.¹⁸ Very recent geological studies have demonstrated the existence of abundant, divalent, volatile metals such as Cd, Zn, Ag, Bi, Cu, and Te in the oxidation state 0 and in the gas phase, close to volcanic eruptions.¹⁸ Nowadays, these metals form oxides when they meet the molecular oxygen present in the atmosphere. However, in the reducing atmosphere of the primeval Earth, there

was no oxygen to oxidize these metals, thus having longer periods to reduce the organic gases present in the atmosphere. This scenario points to an environment with high volcanic activity and with a reducing atmosphere, *i.e.* in the late heavy bombardment age on Earth, about 4.4 Ga ago. These conditions hinder the formation of **16- π -TAzCy** in the gas phase, since the first step is the formation of a C-C bond between **HCN** and **C₂H₂**. This is a very high energy-demanding process which cannot occur in the gas phase conditions mentioned above (see below).

Another possibility could be the formation of a metallic chelate formed from **HCN**, **C₂H₂**, and a metallic atom (Fig. 1c). The formation of such a chelate, namely **Int-M**, would help to catch more units of **HCN** and **C₂H₂** to continue the polymerization around the metallic center, as described below.

Since our Sun is a G2 V star that has barely changed its effective temperature and, therefore, the peak of its spectral energy distribution since the appearance of life on Earth, a primeval molecule that could act as a photosynthetic pigment (for instance **M-18- π -TAzCy**) should show an ultraviolet/visible (UV/Vis) absorption spectrum similar to those of current chlorophylls and bacteriochlorophylls. For comparison purposes, Fig. 2 shows the theoretical UV/Vis absorption spectra in vacuum of chlorophyll a (Chl *a*), bacteriochlorophyll a (BChl *a*), and **M-18- π -TAzCy** with Zn²⁺ and Mg²⁺ as metallic centers. We selected Zn as the metallic center since it is abundant in volcanic eruptions,¹⁸ is a divalent metal, and the spectroscopic characteristics of some tetrapyrrole derivatives complexed with Zn²⁺ are similar to those of the same ligands complexed with Mg²⁺.²⁸ In addition, there are photosynthetic organisms that use Zn-containing BChl *a* as photopigments.^{29,30} On the other hand, Mg²⁺ is the cation of the complexes Chl *a* and BChl *a*. We dubbed these new compounds as Phot0-Zn and Phot0-Mg, respectively.

The overimposed spectra (Fig. 2) show that the weakest absorption peaks of Phot0-Mg and Phot0-Zn are at 562 nm and 548 nm, close to the first and second transitions (Q_y and Q_x, respectively) (the latter is not seen with the set bandwidth) peaks of Chl *a* (586 nm and 557 nm respectively) and the Q_x

peak of BChl *a* (538 nm). The Q_y band of BChl *a*, however, is highly displaced to the red with respect to the other three compounds (727 nm). On the other hand, the B_x and B_y absorption maxima of Chl *a* are at 392 nm and 380 nm respectively, close to the B_y maximum of BChl *a* (373 nm). The most intense peak of BChl *a* (B_x, 336 nm) matches almost exactly with the absorption maxima of Phot0-Mg (339 nm) and Phot0-Zn (332 nm). Regarding the effect of the metal in the Phot0-Mg and Phot0-Zn systems, the Zn²⁺ cation slightly displaces the absorbance maxima to the blue, decreases the intensity in the B band and increases it in the Q band. For simplicity, we will refer to Phot0-Zn as **Phot0** along the manuscript. All in all, this comparison points out that the system **Phot0** could act as a photosynthetic pigment (see below).

2.2 Formation of Phot0

The hypothesis of formation of **Phot0** illustrated by Fig. 1c fits into the geochemical conditions of a rocky exoplanet. Furthermore, its spectroscopic characteristics are similar to those of Chl *a* and BChl *a*. However, since this is a preliminary investigation of the reaction mechanism, it is yet to be demonstrated whether this process is chemically feasible.

The proposed formation of **Phot0** starts with the generation of the intermediate chelate **Int1_{Zn}** (Fig. 3). The first step of the reaction is the formation of the pre-reactive complex C and the subsequent formation of the C-C bond between C₂H₂ and **HCN** (red profile of Fig. 3). That reaction is a radical process that forms the unstable intermediate **Int1** through the transition structure **TS1**. This singlet diradical intermediate in the *s-trans* conformation could either revert to the complex C or evolve into the *s-cis* **Int2** through the rotation of the σ_{C-C} bond (**TS2**). Afterwards, the barrierless association reaction between **Int2** and Zn⁰ leads to the key intermediate **Int1_{Zn}**, the first unit of the system **Phot0**. The geochemical conditions proposed herein would allow the participation of a third partner. In this case the barrierless complexation of the complex C with a Zn atom leads to a slightly more stable complex, **C1_{Zn}**, which evolves into **Int1_{Zn}** through the transition structure **TS1_{Zn}**. In this transition structure the Zn⁰ atom reduces simultaneously the two fragments, favoring the formation of the new C-C bond. In this step two new covalent bonds with the metallic center, Zn-N and Zn-C, are formed in a concerted manner. The latter process (blue profile of Fig. 3) shows a rate-determining step 26.9 kcal mol⁻¹ lower in energy with respect to the previous route.

Although the abundances of **HCN** and **C₂H₂** should have been high in the gas phase of the primeval Earth, we should also consider the presence of water in the volcanic eruptions. In these geochemical conditions, the water is a molecule even more abundant than **HCN** and **C₂H₂** and could lead to competitive chemical pathways. Therefore, we have considered the influence of water both in the formation of the key intermediate **Int1_{Zn}** and in the destruction of Zn. To this aim, we placed 4 water molecules surrounding a Zn atom at a distance of 6 Å and calculated the minimum energy path (MEP) that led to the stable complex **C-Zn-4W**. In this complex just one of the molecules interacts directly with the Zn atom, which forms a

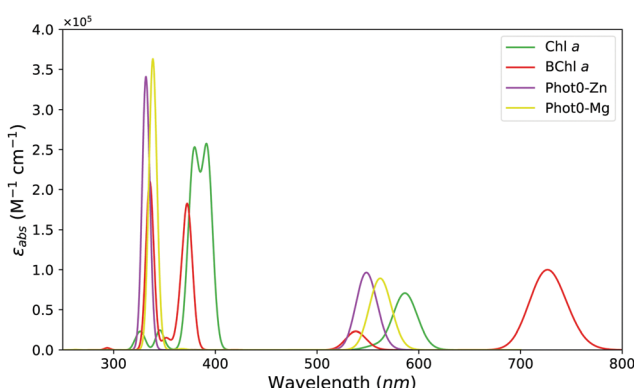


Fig. 2 Theoretical UV/Vis absorption spectra of Chl *a* (green), BChl *a* (red), Phot0-Mg (yellow) and Phot0-Zn (purple) in vacuum. Phytol groups of Chl *a* and BChl *a* are substituted by a methyl group.



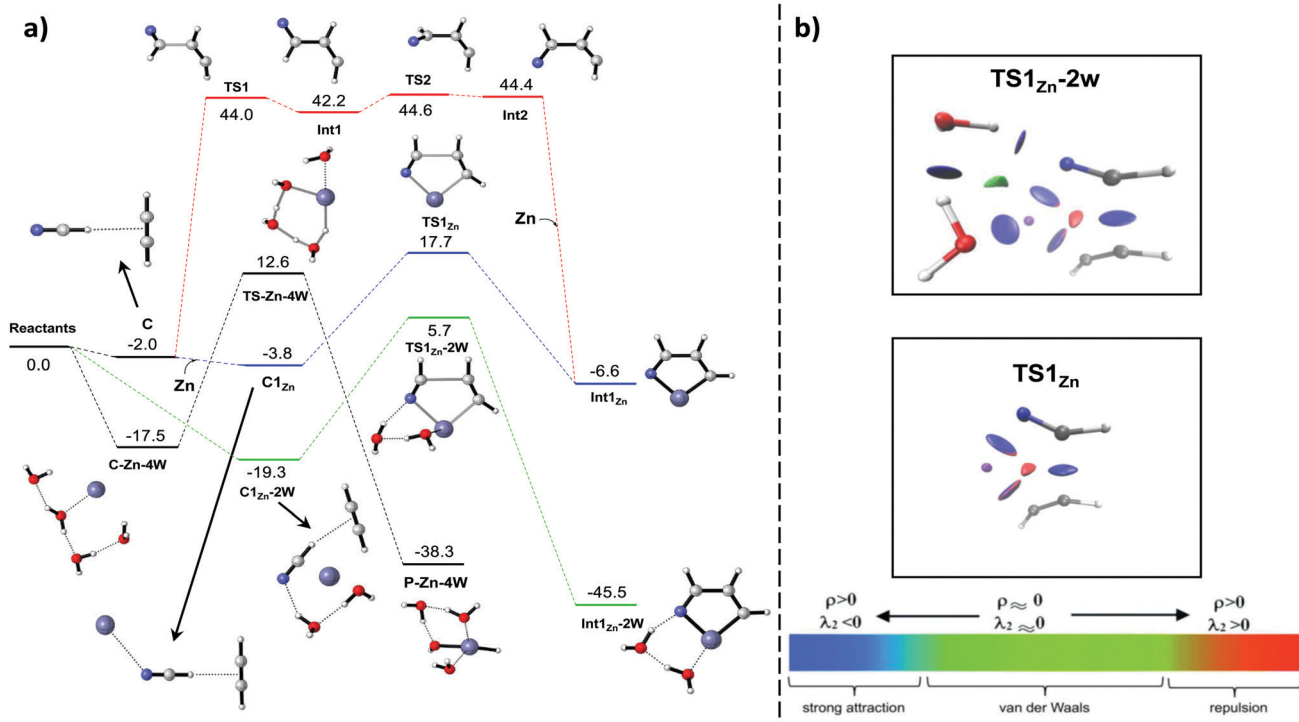


Fig. 3 (a) $E + ZPE$ energy profiles leading to the intermediates **Int1_{Zn}**, **Int1_{Zn}-2W** and **P-Zn-4W**. Energy values are given in kcal mol⁻¹. (b) Non-covalent interactions (NCI) in the transition structures **TS1_{Zn}** and **TS1_{Zn}-2W**.

covalent bond with Zn while there is a proton transfer from other water molecule throughout a concerted cyclic transition structure (**TS-Zn-4W**) that presents an energy barrier of 12.6 kcal mol⁻¹, leading to the formation of **P-Zn-4W** through a highly exothermic process (-38.3 kcal mol⁻¹). The same methodology was carried out by substituting two water molecules for **HCN** and **C₂H₂**. The MEP led to an even more stable complex (**C1_{Zn}-2W**). The latter evolves towards the key intermediate **Int1_{Zn}** coordinated with two water molecules (**Int1_{Zn}-2W**) through the transition structure **TS1_{Zn}-2W**. This process is the most exothermic of all the competitive paths considered (-45.5 kcal mol⁻¹). Regarding kinetics, it is also the most favored process, showing an energy barrier of just 5.7 kcal mol⁻¹. In this process, the water molecules do not participate in the formation of new bonds but generate several stabilizing non-covalent interactions (NCI)³¹ with the Zn atom and the nitrogen of the HCN moiety. The non-covalent interactions of transition structures **TS1_{Zn}** and **TS1_{Zn}-2W** are shown in Fig. 3b. These two stationary points show several identical NCI: Three strong attractive interactions in the bond-forming regions and one destabilizing due to steric repulsions inside the ring that will form. However, **TS1_{Zn}-2W** exhibits four additional stabilizing NCI between water molecules, Zn and nitrogen, contributing to decrease the energy of the system. It is worth pointing out that the very high temperatures of the proposed geochemical conditions¹⁸ would allow all the processes depicted in Fig. 3b to occur, excluding the red profile due to the high energy barriers. Then, part of the Zn in the gas phase should be destroyed by water molecules. However,

considering the high abundance of **HCN** and **C₂H₂** and that the most favoured process both from the kinetic and thermodynamic point of views is the formation of **Int1_{Zn}-2W**, the reaction pathway that should govern this chemistry is the green profile depicted in Fig. 3b.

After the formation of the intermediates **Int1_{Zn}-2W** and/or **Int1_{Zn}**, the oxidized metal serves as a grabber of more electron-rich fragments that helps to increase the molecular weight of the system (see below). To test whether the second step of our chemical hypothesis (Fig. 1c) is viable, we studied the addition of an additional molecule of **C₂H₂** to the intermediates **Int1_{Zn}-2W** and **Int1_{Zn}** (see Fig. 4). The blue and red energy profiles of Fig. 4 show that the insertion of an **C₂H₂** molecule in the Zn–N bond of the intermediates **Int1_{Zn}-2W** and **Int1_{Zn}** is favoured both from the kinetic and the thermodynamic point of view (relative to the intermediates) when water does not participate in the reaction. The two water molecules distort the geometries of the transition structures and intermediates by pulling out the Zn and N atoms from the plane, decreasing the delocalization of the system. This consequence makes the energy barrier that corresponds to the transition structure **TS2_{Zn}** to be submerged with respect the intermediate **Int1_{Zn}** (0.6 kcal mol⁻¹), whereas **TS2_{Zn}** is above the intermediate **Int1_{Zn}-2W** by 8.1 kcal mol⁻¹. Due to this fact, we studied the formation of **Phot0** starting from the intermediate **Int1_{Zn}** instead of **Int1_{Zn}-2W**. Fig. 5 shows the reaction profile for the subsequent additions of three more molecules of **C₂H₂** and three of **HCN** to the complex **Int1_{Zn}**, leading to the formation of the primitive pigment **Phot0** (the mechanism is explained in detail in the



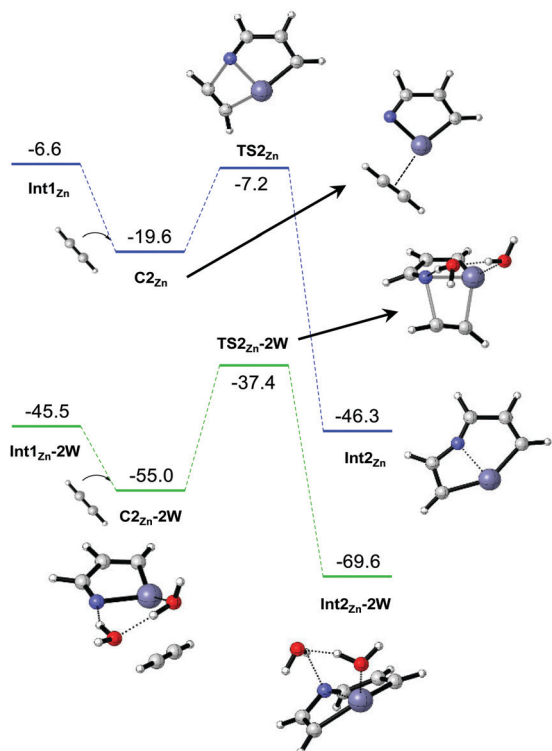


Fig. 4 Same as Fig. 3a, but for the formation of the intermediates **Int2_{Zn}** and **Int2_{Zn}-2W**.

ESI[†]). At a first glance, the whole process is viable thermodynamically. Furthermore, the only process that shows a

barrier above the reactants is the formation of the first intermediate.

The order and position of the additions of **C₂H₂** and **HCN** to the different intermediates could give rise to many complex aromatic heterocycles. However, our aim herein is to study the viability of the formation of the **Phot0** pigment. Even so, a simple frontier molecular orbital analysis of the fragments during key steps of the reaction pathway points out that the strongest interactions are the ones that lead to the formation of **Phot0** (see ESI[†]).

Although the temperatures in the proposed geochemical conditions are very high,¹⁸ they are not high enough as to destroy the reaction intermediates that lead to **Phot0** since the binding energies of the Zn-complexes with the metal are very high (54.2, 80.8, 93.4, 118.4, 103.4 and 101.2 kcal mol⁻¹ for **Int1_{Zn}**, **Int2_{Zn}**, **Int3_{Zn}**, **Int5_{Zn}**, **Int5_{Zn}**, **Int6_{Zn}** and **Int7_{Zn}** respectively. Note that the equilibrium geometry of **Int7_{Zn}** without the Zn atom is that of **Phot0** without the metallic center).

The inclusion of substituted acetylenes and different metals would lead to structural changes in the products and in both, kinetic and thermodynamic data. While relevant, the investigation of these reactions is beyond the scope of this work.

2.3 Chemical evolution of Phot0 into tetrapyrrole systems

Even if tetrapyrrole derivatives are of tremendous importance both in the current biochemistry and in the origin of the photosynthesis, there are hardly any proposals for the formation of these compounds in prebiotic conditions. As it was mentioned above, all the synthetic proposals raised so far involve condensation between highly substituted pyrroles.⁹⁻¹¹

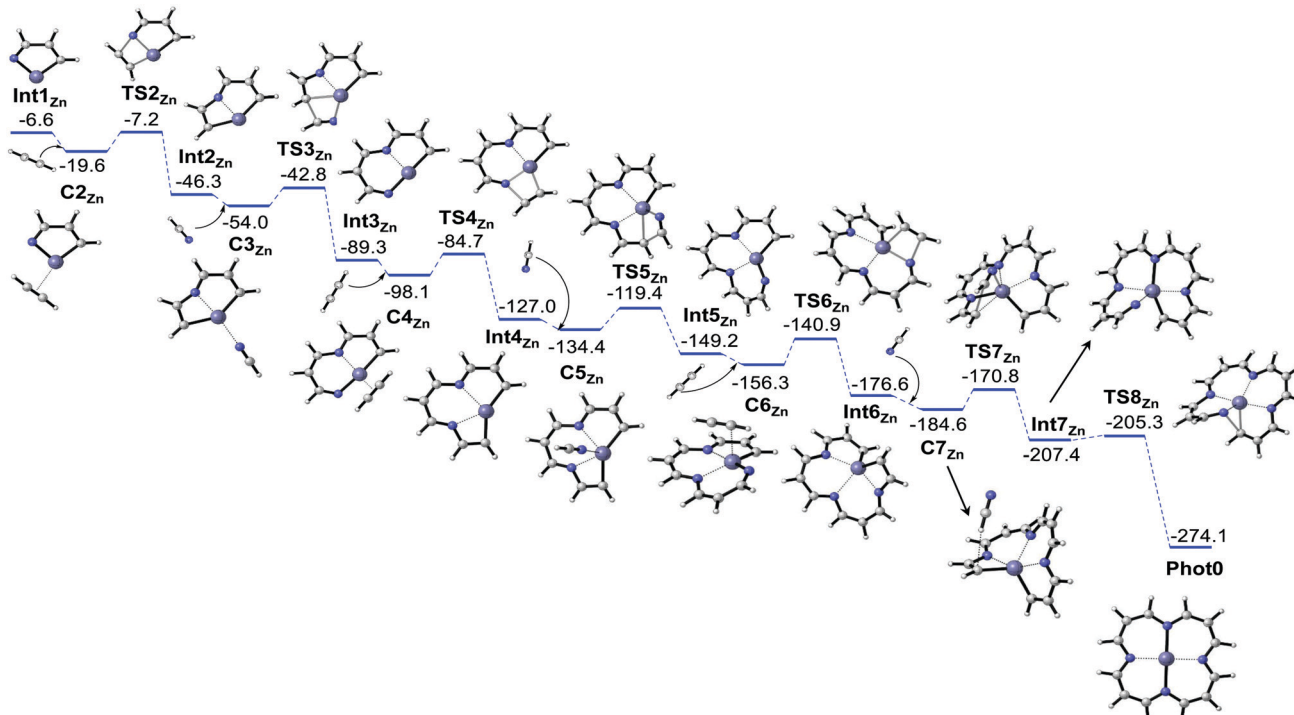


Fig. 5 Same as Fig. 3a, but for the **Phot0** pigment from the intermediate **Int1_{Zn}**.

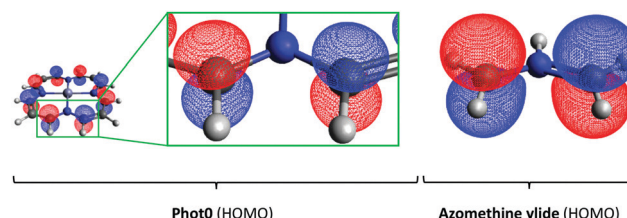


Fig. 6 HOMO orbitals of **Phot0** (left) and the most simple azomethine ylide (right).

Although the proposals on the formation of pyrroles¹³ and their condensation towards tetrapyrroles^{9–12} are robust and viable processes, the complex structure of the raw materials suggests that the concentration of these biomolecules in the environment should have been low. Our new synthetic proposal for tetrapyrroles does not need the previous formation of highly substituted pyrrole derivatives, but subsequent cycloaddition reactions of **Phot0** with highly abundant molecules such as acetylene (C_2H_2) and/or ethylene (C_2H_4).

The inspection of the electronic structure of **Phot0** shows that its highest occupied molecular orbital (HOMO) is identical to that of the HOMO of an azomethine ylide (Fig. 6). The latter is a 1,3-dipole that undergoes 1,3-dipolar cycloadditions with simple dipolarophiles like C_2H_2 and C_2H_4 . In these reactions, the central cation Zn^{2+} traps electron-rich compounds such as these two dipolarophiles and forms stable complexes that undergo concerted 1,3-dipolar cycloadditions (see ESI†). In the subsequent step, the loss of molecular hydrogen from the first intermediate yields the formation of the first unit of pyrrole in the reaction with C_2H_2 . Likewise, the reaction with C_2H_4 leads to the formation of a unit of dihydropyrrole. The addition of C_2H_2 and C_2H_4 at different positions of the intermediates eventually leads to different porphyrins, chlorins, bacteriochlorins, and isobacteriochlorins derivatives without the need of generating complex pyrrole derivatives. The full reactions profiles are gathered in Fig. S4 and explained in ESI.† It should be noted that the cycloaddition reactions with C_2H_2 and C_2H_4 are not viable processes in the geochemical conditions proposed herein due to the high energy barriers found. However, these reactions with substituted acetylenes (and/or ethylenes in this case) should change the reaction profiles, probably lowering the reaction barriers, since the substituted acetylenes and ethylenes are commonly holding electron withdrawing groups that would increase the rate of a direct electron demanding 1,3-dipolar cycloaddition. Anyhow, the full exploration of these reactions with substituted ethylenes and acetylenes lies beyond the scope of this work.

2.4 A new synthetic proposal for complex biomolecules

The geochemical conditions considered herein contribute to widen the environmental situations where key biomolecules could be synthesized in the early Earth and in rocky exoplanets. Within this scenario, complex biomolecules could be formed in the gas phase of volcanic eruptions. Metallic atoms (Zn in this case) in the oxidation state 0 increase notably the rate of

formation of C–C bonds between C_2H_2 and **HCN** (Fig. 3). Furthermore, the initial metallic complex **Int1_{Zn}** serves as a grabber of more electron-rich organic molecules, allowing to increase the chemical complexity.

Most of the syntheses proposed so far for biomolecules in the early Earth consider necessary an aqueous medium. Our new proposal can be applied to the early Earth and any other rocky exoplanet. The probability that raw materials such as C_2H_2 and **HCN** are present in these types of celestial bodies is very high. Furthermore, the metals that can increase the rate of the C–C bond formation between simple electron-rich molecules are abundantly formed in supernovae explosions, remaining available in the interstellar medium. Thus, this situation points to the formation of complex organic compounds on exoplanets just after their formation.

As discussed above, the addition of C_2H_2 and **HCN** to intermediate **Int1_{Zn}** in an order other than that proposed herein could give rise to a multitude of complex heterocycles. In this sense, our proposal can help to broaden the vision on the formation of tholins in the gas phase of other celestial bodies such as Titan.^{32–34}

2.5 **Phot0** as a pigment prior to chlorophylls and bacteriochlorophylls

Within the current theories for the origin of the photosynthesis, it is not yet clear whether the first pigment along the evolution of the photosynthesis was BChl *a* or Chl *a*.³⁵ Using the common ancestry theory as a guideline, we propose that the first pigments should have been simpler than chlorophylls and bacteriochlorophylls, abiotically generated, and maybe used by the earliest forms of proto-organisms.³⁶

The spectroscopic characteristics of **Phot0** (Fig. 2) show that this molecule could have acted as a pigment in a primeval photosynthetic organism. The displacements of the UV/Vis absorption maxima in different pigments allow the adaptation of organisms in different niches.³⁷ This shift is a valuable piece of information to know in what type of environment could have photosynthesis been originated. The photosynthetic organisms that use Chl *a*, such as cyanobacteria, can absorb more amount of light in the red and yellow regions of the visible spectrum in lakes that form dense surface layers.³⁷ On the other hand, organisms that have BChl *a*, such as purple bacteria, grow in anaerobic areas with low visibility, making better use of more energetic light.³⁷ The UV/Vis spectrum of **Phot0** indicates that if a primitive photosynthetic organism used this type of pigment, it would have been able to carry out photosynthesis in low visibility environments. The geochemical conditions in which **Phot0** could have been formed, and its relatively large absorption ability in the most energetic area of the near-UV, would locate this pigment in a deep hydrothermal spring with poor visibility, just the place where life is thought to have originated in our planet.³⁸

The displacement of the pigment bands in the UV/Vis spectrum gives us information about the environment where an organism could thrive. However, the shape of the bands also gives valuable information. While Chl *a* and BChl *a* show wider



bands (see Fig. 2), encompassing a larger spectral region, **Phot0** shows narrower bands specially in the most energetic region. A broad band is indicative of widespread biodiversity, proper of newer evolutionary stages where different organisms use the same pigment in different environments. Likewise, the narrow bands found for **Phot0** are indicative of a very selective pigment for a very specific niche.

The intense band of **Phot0** close to 350 nm could be indicative of a pigment that would flourish in a very old atmosphere without protection. It has been suggested that the earliest photosynthetic reaction centers served as protection for the genetic material against UV radiation.^{39,40} The lack of O₂ in the primitive atmosphere of the early Earth prevented the formation of ozone (O₃), needed to protect the biosphere from the energetic UV radiation. Thus, strong absorption in the near-UV would block a large part of photons harmful to an organism. In this sense, **Phot0** seems to be a suitable pigment for this type of unprotected primitive atmospheres. The information provided by the intense band of **Phot0** (350 nm approximately) agrees with the photosynthetic fitness of this pigment according to our new metric.¹⁷ The latter authors show that **Phot0** would be suitable as a photosynthetic pigment in a reducing atmosphere like that of the early Earth. This analysis would place Chl *a* as the most evolved pigment considered in this study, where the absorption band in the blue region has widened and red-shifted, suited for an organism that does not need high protection against UV radiation.

2.6 Lack of Phot0-like pigments in more evolved photosynthetic systems

Although **Phot0** should have been formed in high concentration in the conditions of an early Earth, we do not see this kind of pigments in more evolved organisms. It has been proposed that the first light-harvesting complexes were similar to that of the proteins CP43 and CP47.¹ Thus, placing this type of complex proteins in a photosynthetic organism that has arisen in the prebiotic phase moves away from the Darwinian evolution of a primitive cellular species. From a chemical point of view, the simplest light-harvesting complex should be a chlorosome-type aggregate, which are multiple pigment molecules stacked up and surrounded by small amounts of carotenoids and quinones, but without a protein supporting them. The lack of a complex protein matrix supports the idea that the first living systems had very simple biomolecules. In this case, simpler oligopeptides than the complex proteins forming the light-harvesting complexes that we know today.

The orientation of the pigments in chlorosomes adopts an almost parallel arrangement between the macrocycles.^{41,42} This arrangement allows the pigments to aggregate through π - π stacking interactions, increasing the interaction energy between them, like it is characteristic of aromatic heterocycles. The different π - π stacking arrangements between aromatic heterocycles have a direct influence on their absorption bands.⁴³ Thus, the H-aggregates, which show a completely parallel arrangement, lead to a spectral blue-shift with respect to the monomer, whereas J-aggregates lead to a red-shift. In the

latter, there is a displacement of the fragments in the direction of the plane of the aromatic compounds. A chlorosome-type aggregate of **Phot0** should show both wider and red-shifted bands, since its **dimer** shows a J-type-aggregate (see Fig. S6, ESI[†]).

Since **Phot0** is smaller than chlorophylls and bacteriochlorophylls, this type of aggregates of **Phot0** should be more labile than that formed with tetrapyrroles. A situation where the interaction energy between the pigments of the light-harvesting complex were not high enough should have forced the organism to spend energy and resources in protecting the complex.

One of the reasons for the existence of chlorosomes may be the need to capture as much light as possible. Another possible reason could be that the π - π stacking interactions without a complex protein protecting the system are not strong enough to keep the pigments linked constantly. If this interaction allows the loss of pigments, the living system should need a huge reservoir of them. The best way to extend the life of these aggregates would be to increase the interaction strength between pigments. This increase could be achieved by substituting **Phot0** with tetrapyrroles, as they show larger aromatic carbon backbones. Therefore, the higher the number of carbons is, the stronger the interaction energy between them becomes.

Another possible reason for the change towards tetrapyrrole derivatives could have been the protection against water. The structure of **Phot0**-like compounds suggests a higher water solubility than that of tetrapyrrole derivatives. A higher solubility in water would reduce the intermolecular forces between aggregates of **Phot0** and would make them susceptible to being lost. These reasons suggest that tetrapyrroles would generate more robust structures. It may be that the next step in the evolution of the pigment was not the direct substitution by chlorophylls or bacteriochlorophylls, but just an increase in the size of the aromatic system. This step could have even remained abiotic, since **Phot0** can react with a multitude of C-C unsaturated compounds to give pyrroles and dihydropyrroles through 1,3-dipolar cycloadditions (Fig. S4, ESI[†]).

3 Conclusions

Based on the theory of common ancestors, we propose that the origin of photosynthesis in the early Earth could have been prior to the use of chlorophylls and bacteriochlorophylls. The novel geochemical conditions that we propose enable the formation of a common primitive pigment that presents spectroscopic characteristics for the development of photosynthesis in typical conditions of deep hydrothermal spring. Furthermore, this divalent metal-coordinated tetraazacycle, baptized as **Phot0**, can be a common precursor to all tetrapyrrole derivatives formed abiotically without the need to involve pyrroles. The proposed synthesis of tetrapyrrole derivatives involves simple molecules like C₂H₂ and HCN close to volcanic eruptions thanks to the ability of neutral metallic atoms such as Zn



to increase the rate of the formation of C-C bonds between these species. Within this scenario, the molecule **Phot0** broadens the vision of the origin of the photosynthesis and makes all the photosynthetic organisms, and others that use the tetrapyrrole derivatives, converge at the same point, as it occurs with the Darwinian theory of the evolution of a primitive cellular species.

4 Materials and methods

Reactive potential energy surface

The calculation of all stationary points was carried out within the density functional theory with the global-hybrid exchange-correlation MN15 density functional method⁴⁴ in combination with the jun-cc-pVTZ basis set.^{45–47} To describe the basis functions for the Zn atom we selected the effective-core potential LANL2DZ.⁴⁸ The MN15 method was chosen because is a very versatile method and resolves well for single and multireference systems.⁴⁴ The latter feature is important in this study since we should compare competitive reaction pathways between open and closed shell species. For instance, the red profile of Fig. 2 shows open shell singlet diradicals and all the stationary points of the blue, black and green profiles of Fig. 2 are closed shell species. In all cases, we checked the stability of the wavefunction for locating the lowest energy solution of the SCF results. We found instabilities for the singlet with diradical character. Thus, the broken-symmetry wavefunction was used in order to destroy the α and β spatial symmetries. These calculations showed eigenvalues of total spin operator ($\langle \hat{S}^2 \rangle$) between 0.9 and 1.1. Frequency calculations were carried out at the same level of theory and the stationary points were characterized as minimum and saddle points by showing none and one imaginary frequency respectively. To ensure that all saddle points were linked to the energy minima, intrinsic reaction coordinate (IRC) analyses were carried out. The barrierless association reactions were checked by placing the equilibrium geometries of the two fragments at 10 Å and then running a downhill IRC calculation until a gradient of zero is reached. All the above-mentioned calculations were carried out with the Gaussian 16 program package.⁴⁹

Calculation of the UV/Vis spectra

The methodology used herein is identical to that used in previous studies of precise calculations of the UV absorption spectrum of Chl *a*.⁵⁰ In this case, to compute the vertical excitation energies we used the double-hybrid B2PLYP within the time-dependent formalism^{51,52} with the def2-TZVP basis set^{53–55} on CAM-B3LYP optimized geometries,⁵⁵ with the inclusion of the dispersion correction D3(BJ).^{56,57} Sirohiwal *et al.*⁵⁰ demonstrated that the double hybrid B2PLYP gives almost identical results to that obtained with DLPNO-STEOM-CCSD calculations. It should be noted that the UV/Vis spectra of the pigments are computed in vacuum and the real displacements and absorbances in a light-harvesting complex change. For this reason, all the comparisons are done over theoretical UV/Vis

spectra. To be able to compare the absorbances between the four compounds, all the bandwidths were set to 0.1 eV. In order to ensure that the transitions cover the whole UV/vis spectral range, we computed 10 roots for Phot0-Zn, Phot0-Mg, Chl *a* and BChl *a* and 20 roots for the dimer of Phot0-Zn.

Calculation of non-covalent interactions

For the calculation of non-covalent interactions (NCI) we used the NCIPILOT 4.0 software⁵⁸ and the visualization of the isosurfaces were carried out with the VMD program⁵⁹.

Conflicts of interest

There are no conflicts to declare.

Acknowledgements

We acknowledge financial support from the Agencia Estatal de Investigación of the Ministerio de Ciencia e Innovación and the European Regional Development Fund “A way of making Europe” through projects CTQ2017-87054-C2-2-P, PID2019-105552RB-C41, PID2019-109522GB-C51, and the Centre of Excellence “María de Maeztu” award to the Centro de Astrobiología (MDM-2017-0737), and from the Instituto Nacional de Técnica Aeroespacial through project S.IGS22001 and a predoctoral contract. We gratefully thank the Research & Technological Innovation and Supercomputing Center of Extremadura (CénitS) for allowing us the use of LUSITANIA computer resources.

Notes and references

- 1 J. M. Olson, *Photosynth. Res.*, 2001, **68**, 95–112.
- 2 J. M. Olson and R. E. Blankenship, *Photosynth. Res.*, 2004, **80**, 373–386.
- 3 D. Mauzerall, *Photosynth. Res.*, 1992, **33**, 163–170.
- 4 H. Hartman, *Orig. Life Evol. Biosph.*, 1998, **28**, 515–521.
- 5 T. E. Meyer, J. J. Van Beeumen, R. P. Ambler and M. A. Cusanovich, in *Origin and Evolution of Biological Energy Conversion*, ed. H. Baltscheffsky, VCH Publishers, New York, 1996, pp. 71–108.
- 6 W. Nitschke, U. Mühlenhoff and U. Liebl, in *Photosynthesis: a Comprehensive Treatise*, ed. A. Raghavendra, Cambridge University Press, Cambridge, 1998, pp. 285–304.
- 7 K. Ruiz-Mirazo, C. Briones and A. de la Escosura, *Chem. Rev.*, 2014, **114**, 285–366.
- 8 S. Granick, *Ann. N. Y. Acad. Sci.*, 1957, **69**, 292–308.
- 9 A. R. M. Soares, M. Taniguchi, V. Chandrasekhar and J. S. Lindsey, *Astrobiology*, 2012, **12**, 1055–1068.
- 10 R. M. Deans, M. Taniguchi, V. Chandrasekhar, M. Ptaszek, D. R. Chambers, A. R. M. Soares and J. S. Lindsey, *New J. Chem.*, 2016, **40**, 6421–6433.
- 11 A. R. M. Soares, M. Taniguchi, V. Chandrasekhar and J. S. Lindsey, *Chem. Sci.*, 2012, **3**, 1963–1974.
- 12 N. Aylward and N. Bofinger, *Orig. Life Evol. Biosph.*, 2005, **4**, 345–368.



13 C. Seitz, W. Eisenreich and C. Huber, *Life*, 2021, **11**, 980.

14 D. T. M. Chung, P. V. Tran, K. Chau Nguyen, P. Wang and J. S. Lindsey, *New J. Chem.*, 2021, **45**, 13302–13316.

15 J. S. Lindsey, *New J. Chem.*, 2021, **45**, 12097–12107.

16 K. C. Nguyen, P. Wang and J. S. Lindsey, *New J. Chem.*, 2021, **45**, 569–581.

17 P. Marcos-Arenal, L. Cerdán, M. Burillo-Villalobos, N. Fonseca-Bonilla, J. G. de la Concepción, M. Ángeles López-Cayuela, F. Gómez and J. A. Caballero, *Astrobiology*, 2022, submitted.

18 E. Mason, P. Wieser, E. Liu, M. Edmonds, E. Ilyinskaya, R. Whitty, T. Mather, T. Elias, P. Nadeau and T. Wilkes, *et al.*, *Commun. Earth Environ.*, 2020, **2**, 79.

19 N. N. Greenwood and A. Earnshaw, *Chemistry of the Elements*, Butterworth-Heinemann, Oxford, Boston, 2006.

20 J. H. Lacy, I. Evans, J. Neal, J. M. Achtermann, D. E. Bruce, J. F. Arens and J. S. Carr, *Astrophys. J.*, 1989, **342**, L43.

21 L. E. Snyder and D. Buhl, *Astrophys. J.*, 1971, **163**, L47.

22 L. M. Mukhin, *Orig. Life Evol. Biosph.*, 1976, **7**, 355–368.

23 P. Rimmer and S. Rugheimer, *Icarus*, 2019, **329**, 124–131.

24 M. Ferus, F. Pietrucci, A. M. Saitta, O. Ivanek, A. Knizek, P. Kubelk, M. Krus, L. Juha, R. Dudzak, J. Dostál, A. Pastorek, L. Petera, J. Hrnčirova, H. Saeidfirozeh, V. Shestivská, J. Sponer, J. E. Sponer, P. Rimmer, S. Civiš and G. Cassone, *Astron. Astrophys.*, 2019, **626**, A52.

25 H. Genda, R. Brasser and S. Mojzsis, *Earth Planet. Sci. Lett.*, 2017, **480**, 25–32.

26 S. A. Benner, E. A. Bell, E. Biondi, R. Brasser, T. Carell, H.-J. Kim, S. J. Mojzsis, A. Omran, M. A. Pasek and D. Trail, *ChemSystemsChem*, 2020, **2**, e1900035.

27 K. J. Zahnle, R. Lupu, D. C. Catling and N. Wogan, *Planetary Sci. J.*, 2020, **1**, 11.

28 M. Taniguchi and J. S. Lindsey, *Photochem. Photobiol.*, 2021, **97**, 136–165.

29 M. Kobayashi, M. Yamamura, M. Akiyama, H. Kise, K. Inoue, M. hara, N. Wakao, K. Yahara and T. Watanabe, *Anal. Sci.*, 1998, **14**, 1149–1152.

30 N. Wakao, N. Yokoi, N. Isoyama, A. Hiraishi, K. Shimada, M. Kobayashi, H. Kise, M. Iwaki, S. Itoh and S. Takaichi, *Plant Cell Physiol.*, 1996, **37**, 889–893.

31 E. R. Johnson, S. Keinan, P. Mori-Sánchez, J. Contreras-García, A. J. Cohen and W. Yang, *J. Am. Chem. Soc.*, 2010, **132**, 6498–6506.

32 M. S. Gudipati, R. Jacovi, I. Couturier-Tamburelli, A. Lignell and M. Allen, *Nat. Commun.*, 2013, **4**, 1648.

33 D. Dubois, N. Carrasco, M. Petrucciani, L. Vettier, S. Tigrine and P. Pernot, *Icarus*, 2019, **317**, 182–196.

34 Z. Perrin, N. Carrasco, A. Chatain, L. Jovanovic, L. Vettier, N. Ruscassier and G. Cernogora, *Processes*, 2021, **9**, 965.

35 R. E. Blankenship, *Origin and Evolution of Photosynthesis*, John Wiley Sons, Ltd, 2002, ch. 11, pp. 220–257.

36 J. A. Mercer-Smith and D. C. Mauzerall, *Photochem. Photobiol.*, 1984, **39**, 397–405.

37 S. Seager, E. Turner, J. Schafer and E. Ford, *Astrobiology*, 2005, **5**, 372–390.

38 B. Damer and D. Deamer, *Astrobiology*, 2020, **20**, 429–452.

39 A. Y. Mulkidjanian, *Photosynth. Res.*, 1997, **51**, 27–42.

40 A. Y. Mulkidjanian, E. V. Koonin, K. S. Makarova, S. L. Mekhedov, A. Sorokin, Y. I. Wolf, A. Dufresne, F. Partensky, H. Burd, D. Kaznadzey, R. Haselkorn and M. Y. Galperin, *Proc. Natl. Acad. Sci. U. S. A.*, 2006, **103**, 13126–13131.

41 J. Pšenčík, S. J. Butcher and R. Tuma, in *Chlorosomes: Structure, Function and Assembly*, ed. M. F. Hohmann-Marriott, Springer Netherlands, Dordrecht, 2014, pp. 77–109.

42 R. G. Saer and R. E. Blankenship, *Biochem. J.*, 2017, **474**, 2107–2131.

43 N. J. Hestand and F. C. Spano, *Acc. Chem. Res.*, 2017, **50**, 341–350.

44 H. S. Yu, X. He, S. L. Li and D. G. Truhlar, *Chem. Sci.*, 2016, **7**, 5032–5051.

45 E. Papajak, H. R. Leverentz, J. Zheng and D. G. Truhlar, *JCTC*, 2009, **5**, 1197–1202.

46 T. H. Dunning, Jr., K. A. Peterson and A. K. Wilson, *JChPh*, 2001, **114**, 9244.

47 B. Prascher, D. E. Woon, K. A. Peterson and T. H. Dunning, Jr., *TCA*, 2011, **128**, 69.

48 P. J. Hay and W. R. Wadt, *J. Chem. Phys.*, 1985, **82**, 270–283.

49 M. J. Frisch, G. W. Trucks, H. B. Schlegel, G. E. Scuseria, M. A. Robb, J. R. Cheeseman, G. Scalmani, V. Barone, G. A. Petersson, H. Nakatsuji, X. Li, M. Caricato, A. V. Marenich, J. Bloino, B. G. Janesko, R. Gomperts, B. Mennucci, H. P. Hratchian, J. V. Ortiz, A. F. Izmaylov, J. L. Sonnenberg, D. Williams-Young, F. Ding, F. Lipparini, F. Egidi, J. Goings, B. Peng, A. Petrone, T. Henderson, D. Ranasinghe, V. G. Zakrzewski, J. Gao, N. Rega, G. Zheng, W. Liang, M. Hada, M. Ehara, K. Toyota, R. Fukuda, J. Hasegawa, M. Ishida, T. Nakajima, Y. Honda, O. Kitao, H. Nakai, T. Vreven, K. Throssell, J. A. Montgomery, Jr., J. E. Peralta, F. Ogliaro, M. J. Bearpark, J. J. Heyd, E. N. Brothers, K. N. Kudin, V. N. Staroverov, T. A. Keith, R. Kobayashi, J. Normand, K. Raghavachari, A. P. Rendell, J. C. Burant, S. S. Iyengar, J. Tomasi, M. Cossi, J. M. Millam, M. Klene, C. Adamo, R. Cammi, J. W. Ochterski, R. L. Martin, K. Morokuma, O. Farkas, J. B. Foresman and D. J. Fox, *Gaussian 16 Revision C.01*, Gaussian Inc., Wallingford CT, 2016.

50 A. Sirohiwal, R. Berraud-Pache, F. Neese, R. Izsák and D. A. Pantazis, *J. Phys. Chem. B*, 2020, **124**, 8761–8771.

51 S. Grimme, *J. Chem. Phys.*, 2006, **124**, 034108.

52 S. Grimme and F. Neese, *J. Chem. Phys.*, 2007, **127**, 154116.

53 F. Weigend and R. Ahlrichs, *Phys. Chem. Chem. Phys.*, 2005, **7**, 3297–3305.

54 F. Weigend, *Phys. Chem. Chem. Phys.*, 2006, **8**, 1057–1065.

55 A. Hellweg, C. Hättig, S. Höfener and W. Klopper, *Theor. Chem. Acc.*, 2007, **117**, 587–597.

56 S. Grimme, J. Antony, S. Ehrlich and H. Krieg, *J. Chem. Phys.*, 2010, **132**, 154104.

57 S. Grimme, S. Ehrlich and L. Goerigk, *J. Comput. Chem.*, 2011, **32**, 1456–1465.

58 R. A. Boto, F. Peccati, R. Laplaza, C. Quan, A. Carbone, J.-P. Piquemal, Y. Maday and J. Contreras-Garcia, *J. Chem. Theory Comput.*, 2020, **16**(7), 4150–4158.

59 W. Humphrey, A. Dalke and K. Schulten, *J. Mol. Graph.*, 1996, **14**, 33–38.

